Applied Catalysis B: Environmental 84 (2008) 241–250

Contents lists available at ScienceDirect

Applied Catalysis B: Environmental

journal homepage: www.elsevier.com/locate/apcatb

Stability of hexaaluminate-based catalysts for high-temperature catalytic combustion of methane

Erik Elm Svensson *, Magali Boutonnet, Sven G. Järås

KTH-Royal Institute of Technology, School of Chemical Science and Engineering, Chemical Technology, Teknikringen 42, SE-10044 Stockholm, Sweden

ARTICLE INFO

Article history:
Received 24 April 2007
Received in revised form 28 March 2008
Accepted 5 April 2008
Available online 11 April 2008

Keywords:
Catalytic combustion
Hexaaluminate
Methane
$LaMnO_3$
CeO_2
Microemulsion

ABSTRACT

Lanthanum hexaaluminate with a nominal composition of $LaAl_{11}O_{18}$ was used to support 20 wt.% of $LaMnO_3$ and CeO_2. $LaAl_{11}O_{18}$ was prepared through co-precipitation of metal nitrates within the water phase of an isooctane/CTAB/1-butanol microemulsion. The stabilities of the prepared catalysts were assessed by measuring the activities for combustion of methane before and after aging at 1000 °C for 100 h in air with 10 vol.% H_2O. The activities were compared with $LaMnAl_{11}O_{19}$, due to its well-documented stability. It was shown that by using hydrothermal treatment of the microemulsion, a significantly higher surface area was obtained for the $LaAl_{11}O_{18}$. For $LaMnO_3$, the reference support (Al_2O_3) was shown to be superior to $LaAl_{11}O_{18}$ as support, both in terms of activity and stability. Reactions between $LaMnO_3$ and support were observed for all supports included in the study. For CeO_2, $LaAl_{11}O_{18}$ was superior to Al_2O_3 as support. Deactivations of the CeO_2 catalysts were linked to crystal growth of CeO_2. LMHA deactivated strongly during aging; $LaMnO_3$ on Al_2O_3 and several of the catalysts with CeO_2 supported on $LaAl_{11}O_{18}$ showed a much more stable behavior.

1. Introduction

Catalytic combustion, or heterogeneous combustion, has been extensively investigated in recent years. The interest has mainly been raised by more stringent environmental legislation concerning emissions of hazardous substances such as NO_X, CO and hydrocarbons. Compared to homogeneous combustion, catalytic combustion can stabilize the combustion while avoiding reaching the threshold temperature for thermal-NO_X formation. Catalytic combustion has for this reason emerged as a very promising technique for gas-turbine applications [1–3]. The catalyst in a gas-turbine combustor has to withstand continuous operation for at least 1 year under very demanding conditions [4]. Material development is therefore one of the key issues in the development of catalytic combustion for gas turbines [1].

One of the most promising groups of materials for high-temperature applications is hexaaluminates [5,6]. Hexaaluminates are well known for their extreme sintering resistance originating from their layered crystal structure, which result in the formations of plate-shaped crystals with high aspect ratios [6]. Hexaaluminates can be represented by the general formula $AB_XAl_{12-X}O_{19}$, where A represents an alkaline, alkaline-earth or rare-earth metal ion and B a transition-metal ion with similar size and charge as aluminium. Substituting a few of the aluminium ions with transition-metals ions can substantially increase the oxidation activity of the material while retaining a similar sintering resistance compared to the non-substituted material [6]. The highest activities have been shown by hexaaluminates with manganese substitution [7]. However, it is currently unknown if manganese-substituted hexaaluminates, prepared by conventional methods, are active enough to ignite the fuel mixture after a palladium-containing ignition segment under gas-turbine conditions. It is therefore of interest to investigate alternative routes to increase the activity of the hexaaluminate, while taking full advantage of its stability. One way to increase the activity of the hexaaluminate is to disperse a more active component on its surface. In this way the thermal stability of the support can be utilized to protect the active material from sintering. However, great care has to be taken in the choice of the active component. First of all, the support has to be compatible with the active component, i.e. no interactions between the two should occur that result in formations of less active species and/or induce sintering of the support. Secondly, the active material should have as low vapor pressure as possible in order to minimize the loss of material through vaporization.

* Corresponding author. Tel.: +46 8 7908243; fax: +46 8 108579.
E-mail address: eelm@ket.kth.se (E.E. Svensson).

0926-3373/$ – see front matter © 2008 Elsevier B.V. All rights reserved.
doi:10.1016/j.apcatb.2008.04.002

Two promising active materials for methane combustion are perovskites (e.g. $LaMnO_3$) [8,9] and ceria (CeO_2) [5,10]. Both $LaMnO_3$ and CeO_2 are active for methane combustion, but have strong tendencies to sinter if subjected to temperatures above 900 °C [11,12] and would therefore potentially benefit from being supported.

Zwinkels et al. [13] and Marti et al. [14] used hexaaluminate ($LaAl_{11}O_{18}$) as support for perovskite ($LaCrO_3$ and $La_{0.8}Sr_{0.2}CrO_3$, respectively). Both authors found that the perovskites supported on hexaaluminate showed lower activities than if they were supported on the reference supports (γ-Al_2O_3 and $LaAlO_3$, respectively). In both cases the lower activities might be explained by structural differences of the supports used. The hexaaluminates used had lower surface area compared to alumina and smaller pores compared to $LaAlO_3$. Furthermore, both authors chose rather low calcination temperatures of the hexaaluminates (1000 and 1100 °C, respectively) before adding the perovskites, which might have caused interactions between the partly amorphous supports and the perovskites. In previous work [15] our group has shown that it is possible to increase both the surface area and pore size of lanthanum hexaaluminate by using the microemulsion technique [16] combined with hydrothermal treatment. By adding perovskite ($LaMnO_3$) to these materials, substantially higher activities were obtained compared to adding $LaMnO_3$ on a hexaaluminate prepared by an aqueous method.

Zarur et al. [17] used the microemulsion technique to prepare a hexaaluminate ($BaAl_{12}O_{19}$) and added CeO_2 to the surface of the hexaaluminate-precursor particles while they still were suspended in the microemulsion. This catalyst showed excellent activity, which was reported to be retained after aging at 1100 °C in 10 vol.% steam in air. The duration of the aging was however not reported. The authors attributed the high activity to the small CeO_2 crystallites formed by using the microemulsion technique. Other authors have found that the crystallite size of CeO_2 is important for the methane combustion activity [10]. Furthermore, doping of CeO_2 with zirconium and lanthanum have shown to have strongly promoting effects for the activities and stabilities, due to increased reducibility and prevention of crystal growth [12,18].

The objective of this work was to investigate the activities and stabilities of $LaMnO_3$ and CeO_2 supported on lanthanum hexaaluminate (LHA), with a nominal composition of $LaAl_{11}O_{18}$, as catalysts for high-temperature catalytic combustion of methane. Most previous studies have assessed the stabilities of the catalysts by exposing the materials to high temperatures in dry atmosphere for only a few hours. During combustion, a substantial amount of water vapor is produced, which is well known to accelerate sintering for many materials [19]. Aging for extended periods in humid air was for this reason included in the present study. The preparation method of the lanthanum hexaaluminate was chosen based on promising results previously obtained with $LaMnO_3$ supported on lanthanum hexaaluminate [15]. The preparation method was varied in order to test the impacts that the structural properties of the supports and the dispersions of the active components have on the activities and stabilities of the catalysts. Two alternative preparation methods of LHA were tested. One with high surface area, obtained by hydrothermal treatment of the microemulsion and one more crystalline with lower surface area, directly recovered from the microemulsion. Two impregnation methods were used to apply $LaMnO_3$ and CeO_2 to the surface of the LHA: the incipient wetness technique and surface precipitation. Manganese-substituted lanthanum hexaaluminate (LMHA) was included in the study for comparison purposes since it has been reported to be one of the most stable active materials.

2. Experimental

2.1. Catalyst preparation

Lanthanum hexaaluminate (LHA) was prepared using the microemulsion technique. The compositions of oil phase (53.9 wt.% isooctane), surfactant (13.5 wt.% CTAB), co-surfactant (12.0 wt.% 1-butanol) and water phase (20.6 wt.%) in the microemulsions were similar as used by Palla et al. [20], replacing *n*-octane with isooctane. In Fig. 1, a schematic illustration of the preparation procedure is shown. Three microemulsions with the same phase compositions were used with different components dissolved in the water phases. Microemulsion 1 contained $La(NO_3)_3{\cdot}6H_2O$ and $Al(NO_3)_3{\cdot}9H_2O$, with a concentration of La and Al in the water phase of 0.15 and 1.65 M, respectively. This microemulsion was slowly added to Microemulsion 2, containing four times the stoichiometric amount of $(NH_4)_2CO_3$ (0.8 M) to form lanthanum carbonate. Microemulsion 3, containing an undiluted aqueous solution of NH_3 (28–30%), was used to keep the pH-value constant at 8–9. After aging the precipitated particles for 4 h, one batch was directly recovered (termed LHA). One batch was before recovery subjected to hydrothermal treatment in an autoclave at 150 °C for 20 h in nitrogen atmosphere (termed LHA-150). The suspended particles, from both batches, were recovered by means of centrifugation and washed with a chloroform/methanol mixture (1:1 based on volume) once and methanol once in order to remove most of the surfactant. The particles were dried at 60 °C and thereafter ground in a mortar. The materials were calcined for 4 h at 1200 °C with the ramping speed set to 2 °C/min, dwelling at 200 °C for 4 h and a slower ramping speed of 0.5 °C/min from 200 to 400 °C in order to remove the remaining surfactant in a gentle fashion.

For comparison purposes was also a commercial alumina (Sasol, PURALOX HP-14/150) used as support. The alumina was calcined at 1000 °C for 1 h prior to impregnation with active components.

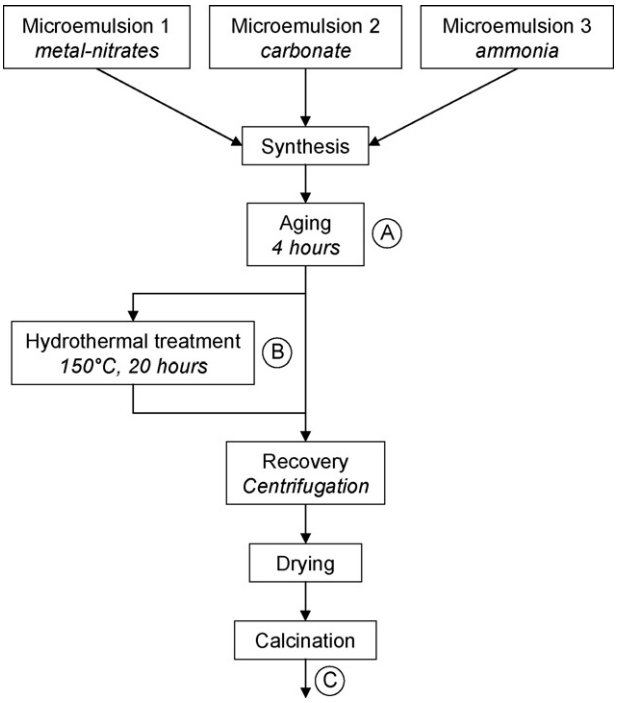

Fig. 1. Schematic illustration of the preparation procedure for lanthanum hexaaluminate. The letters A–C indicate alternative points in the procedure to introduce the active materials CeO_2 and $LaMnO_3$.

The active components ($LaMnO_3$ and CeO_2) were added up to an amount of 20 wt.%, based on the total weight of the support and the active material, by adding $La(NO_3)_3{\cdot}6H_2O$ and $Mn(NO_3)_2$ (aqueous solution, 45–50 wt.%), in the case of $LaMnO_3$, and $Ce(NO_3)_3{\cdot}6H_2O$, in the case of CeO_2. The active components were introduced at three alternative points in the preparation, indicated by the letters A, B and C in Fig. 1. Alternative A and B (surface precipitation) involved adding a fourth microemulsion to the aged LHA precursor (A) or to the hydrothermally treated LHA precursor (B). The fourth microemulsion, with the same phase composition as the other microemulsions, contained cerium nitrate in the water phase (Ce = 1.65 M). While adding the fourth microemulsion, further adding of Microemulsion 3 (NH_3) was needed in order to keep the pH-value at an appropriate level (pH > 8). Alternative C indicates impregnation after calcination of the LHA precursor, following the incipient wetness technique using an aqueous solution of the metal nitrates. The impregnation of alumina also followed the incipient wetness technique. After impregnation, all materials were calcined at 1000 °C for 4 h.

Manganese-substituted lanthanum hexaaluminate (LMHA) was prepared using an aqueous co-precipitation method as used by Ersson et al. [21] and calcined at 1200 °C for 4 h.

All chemicals used in the catalyst preparations were supplied by Aldrich and were of ACS reagent grade. The water used was in all cases deionized water (Milli-Q).

2.2. Activity tests of supported catalysts

The catalyst materials were coated onto cordierite monoliths (Corning, 400 cpsi) with 14 mm diameter and 10 mm length. Slurries, consisting of ethanol and catalyst powder (20 wt.% catalyst), were prepared by ball-milling for 24 h. The monoliths were dipped in the slurries and the excess slurry was removed by blowing compressed air through the monolith channels, after which the monoliths were dried at 90 °C for 2 h. The dipping/drying procedure was repeated until catalyst loadings of 20 wt.% of the total weight (monolith and catalyst material) were reached. The coated monoliths were thereafter calcined at 1000 °C for 1 h.

The activities of the monolith catalysts were tested in a tubular reactor operating at atmospheric pressure, consisting of a quartz glass tube inserted in an electrically heated furnace. Two thermocouples were used: one upstream and one downstream of the catalyst. The temperatures directly in front of the catalysts were used to represent the catalyst temperatures in the tests. It should be stressed that these temperatures were only used to compare the activities of the different catalysts. Comparison with literature data, where the actual catalyst temperature was measured, should be done with care due to the highly exothermic reactions occurring. The reactant gas mixture consisted of 1.5 vol.% methane in air, giving a space velocity of 100,000 h^{-1} (based on the total volume of the monolith) at NTP. The temperature of the furnace was ramped from 300 to 900 °C twice (5 °C/min). The first ramp was used to condition the catalysts in the reaction atmosphere, whereas the second was used to generate ignition curves that were used to compare the activities of the catalysts. The gas exiting the reactor was analyzed using an on-line gas chromatograph (Varian 3800) equipped with a thermal conductivity detector (TCD).

2.3. Catalyst aging

The influences of aging were investigated by testing the activities before and after subjecting the monolith catalysts to aging at 1000 °C for 100 h in air with 10 vol.% H_2O. A powder sample of each catalyst material, originating from the dried slurries used for the coating procedure, was aged simultaneously with the monoliths. These samples were used for characterization.

2.4. Characterization

Surface area and pore size distribution were measured by nitrogen adsorption at liquid N_2 temperature using a Micromeretics ASAP 2010 instrument. The crystal phases were determined by X-ray diffraction (XRD), using a Siemens Diffractometer D5000 scanning 2θ from 10° to 70° using Ni-filtered Cu Kα radiation. Crystal phases were identified by comparing the diffractograms with powder diffraction files (ICDD/JCPDS, PDF-2). Temperature programmed reduction (TPR) was performed with hydrogen using a Micromeretics Autochem 2910 equipped with a TCD. Approximately 0.3 g of catalyst was used for each TPR analysis. The catalyst materials were pre-treated with 5 vol.% O_2 in He at 800 °C for 30 min. The samples were reduced with 5 vol.% H_2 in Ar (30 cm^3/min) heating 10 °C/min from room temperature to 800 °C (for $LaMnO_3$) and 950 °C (for CeO_2), dwelling at the maximum temperature for 30 min. The size and shape of the particles were investigated by transmission electron microscopy (TEM) using a JEOL JSM-2100F. Elemental compositions were analyzed using an Oxford Instruments INCA Energy EDX.

3. Results and discussion

3.1. Structural properties

A summary of the structural properties of the supports, before impregnation with active materials including identification codes used throughout the text, are shown in Table 1. Calcination of alumina (termed Al_2O_3) at 1000 °C induced formation of the high-temperature phase θ-Al_2O_3, which is in line with literature data [1]. As shown in previous work [15], by subjecting the particles suspended in the microemulsion to hydrothermal treatment, a higher final surface area was obtained for the support (termed LHA-150) compared to the non-treated support (termed LHA). The major crystal phase in both LHA and LHA-150 were $LaAlO_3$, which is in line with previous reports after calcination at 1200 °C [22,23]. In Fig. 2, parts of the diffractograms for LHA and LHA-150 are shown. The intensity of the $LaAlO_3$ reflection (dashed line) was higher for LHA-150 compared to LHA, at the same time as the

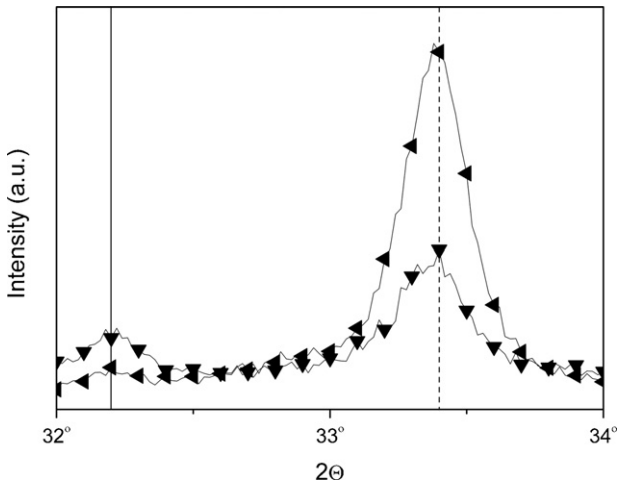

Fig. 2. X-ray diffractograms for the lanthanum hexaaluminate (LHA) supports after calcination at 1200 °C. Non-hydrothermally treated (LHA, ▼) and hydrothermally treated (LHA-150, ◀). The solid line indicates a $LaAl_{11}O_{18}$ reflection and the dashed line indicates a $LaAlO_3$ reflection.

Table 1
Summary of the structural properties of the supports

Identification code[a]	Nominal composition	Crystal phase (XRD)[b]	Average pore size (nm)	Surface area (m^2/g)
Al_2O_3	Al_2O_3	θ-Al_2O_3	34	111
LHA	$LaAl_{11}O_{18}$	LAP, HA	41	19
LHA-150	$LaAl_{11}O_{18}$	LAP, (HA)	44	47
LMHA	$LaMnAl_{11}O_{19}$	HA	17	17

All materials were calcined at 1200 °C for 4 h except Al_2O_3 which was calcined at 1000 °C for 1 h.
[a] LHA = lanthanum hexaaluminate, LMHA = manganese-substituted lanthanum hexaaluminate. The number (150) indicates the temperature during hydrothermal treatment of the particles suspended in the microemulsion.
[b] Crystal phases are listed in order of intensity. Brackets indicate trace amount. HA = hexaaluminate, LAP = $LaAlO_3$.

lanthanum hexaaluminate reflection (solid line) was smaller. An increased amount of $LaAlO_3$ indicates that more alumina was present in LHA-150. Since no α-Al_2O_3 was detected in this sample, this is likely explaining the higher surface area observed for LHA-150 compared to LHA. Manganese-substituted lanthanum hexaaluminate (termed LMHA) showed only reflections originating from hexaaluminate, which also is in line with the literature after calcination at 1200 °C [22].

The name lanthanum hexaaluminate (LHA) in the following will be used to refer to the supports with the nominal composition of $LaAl_{11}O_{18}$, indicating the target crystal structure. The name LHA will be used to group the above-mentioned supports without considering the actual contents of lanthanum hexaaluminate and $LaAlO_3$ in each particular material.

A summary of the structural properties of the materials after impregnation with $LaMnO_3$ and CeO_2, before and after aging at 1000 °C for 100 h in humid air including identification codes used throughout the text, is shown in Table 2.

Impregnation with $LaMnO_3$ did not significantly change the crystal phases of the supports according to XRD. However, changes in the crystal structure of $LaMnO_3$ were detected due to interactions with the supports, even if the presence of $LaAlO_3$ in the LHA supports complicated the detection. $LaAlO_3$ and $LaMnO_3$ are isostructural with only small differences in space groups, which cause the XRD reflections from the two phases to coincide with only a small shift. Furthermore, the two phases can form solid solutions ($LaAl_{1-X}Mn_XO_3$), which will give intermediate reflections [24]. Indeed, intermediate reflections originating from $LaAl_{1-X}Mn_XO_3$ were identified for LMP/Al_2O_3 as seen in Fig. 3a, indicating that a solid solution was formed. Also LMP/LHA and LMP/LHA-150 showed signs of the formations of $LaAl_{1-X}Mn_XO_3$ solid solutions as seen in Fig. 3b and c, respectively. The $LaAl_{1-X}Mn_XO_3$ peaks were, in these cases, not resolved due to the close proximity to the $LaAlO_3$ peaks, originating from the supports. However, since the reflection peaks from the $LaAl_{1-X}Mn_XO_3$ solid solutions were wider than the reflections from $LaAlO_3$, they were possible to identify in shifts close to that of LMP/Al_2O_3. The amounts of Al in the formed $LaAl_{1-X}Mn_XO_3$ solid solutions were further investigated by TPR analyses, presented in the redox properties Section 3.2 below.

After aging the $LaMnO_3$ catalysts at 1000 °C for 100 h in humid air, all catalysts showed shifts of the $LaAl_{1-X}Mn_XO_3$ peaks in the diffractograms toward $LaAlO_3$ (Fig. 3), indicating that more Al-rich solid solutions were formed. For the LHA-supported catalysts, the XRD reflections of $LaAl_{1-X}Mn_XO_3$ were no longer distinguishable from the reflections of $LaAlO_3$. All supports experienced major changes in the crystal structure during aging. For LMP/Al_2O_3, the aging resulted in the formation of hexaaluminate as the major crystalline phase (Fig. 3a), indicating major interaction between the support and active material. However, a part of the poorly crystalline θ-Al_2O_3 was still retained, which gave the material a high surface area. This was probably due to the present lanthanum, which is well known for its ability to stabilize alumina by inhibiting the phase transition into α-Al_2O_3 [19]. As seen in Fig. 3b and c, the amounts of hexaaluminate in LMP/LHA and LMP/LHA-150 increased and the amounts of $LaAlO_3$ decreased. Since the supports in these cases were pre-calcined at 1200 °C, it is rather surprising that aging at 1000 °C would cause these changes in the morphology. An explanation for this could be the manganese present, which has previously been shown to increase the mobility of lanthanum in the alumina lattice and therefore induce formation of hexaaluminate at temperatures as low as 900 °C [22]. The changes were more pronounced for the hydrothermally treated sample (LMP/LHA-150), which could explain the large drop in surface area for this material.

Impregnation with ceria (CeO_2), using the incipient wetness technique, did not significantly change the crystal phases of the supports. In fact, no interactions between CeO_2 and supports were detected with XRD. The two impregnation methods, incipient wetness (IW) and surface precipitation (SP), gave very different results in terms of phases present and surface areas (Table 2). This can be attributed to the fact that the supports, in the case of surface

Table 2
Identification codes and summary of the structural properties for all catalysts used in the activity tests before and after aging at 1000 °C for 100 h in air with 10 vol.% H_2O

Identification code[a]	Nominal composition	Crystal phase (XRD)[b]		Surface area (m^2/g)	
		Fresh	Aged	Fresh	Aged
LMP/Al_2O_3	20% $LaMnO_3$, 80% Al_2O_3	LAM[c], θ-Al_2O_3	HA, LAM, θ-Al_2O_3	83	61
LMP/LHA	20% $LaMnO_3$, 80% $LaAl_{11}O_{18}$	LAP, LAM[c], HA	HA, LAP	20	18
LMP/LHA-150	20% $LaMnO_3$, 80% $LaAl_{11}O_{18}$	LAP, LAM[c], (HA)	LAP, HA	41	23
Ce/Al_2O_3	20% CeO_2, 80% Al_2O_3	CeO_2, θ-Al_2O_3	CeO_2, α-Al_2O_3	72	34
Ce/LHA-IW	20% CeO_2, 80% $LaAl_{11}O_{18}$	CeO_2, LAP, HA	CeO_2, LAP, HA	21	19
Ce/LHA-SP	20% CeO_2, 80% $LaAl_{11}O_{18}$	CeO_2, θ-Al_2O_3	CeO_2, θ-Al_2O_3	97	51
Ce/LHA-150-IW	20% CeO_2, 80% $LaAl_{11}O_{18}$	LAP, CeO_2, (HA)	LAP, CeO_2, (HA)	46	41
Ce/LHA-150-SP	20% CeO_2, 80% $LaAl_{11}O_{18}$	CeO_2, LAP, θ-Al_2O_3	CeO_2, LAP, θ-Al_2O_3	69	46
LMHA	$LaMnAl_{11}O_{18}$	HA	HA	17	17

[a] LMP = $LaMnO_3$, Ce = CeO_2, LHA = lanthanum hexaaluminate, LMHA = manganese-substituted lanthanum hexaaluminate. The number (150) indicates the temperature during hydrothermal treatment. IW (incipient wetness) and SP (surface precipitation) indicate the methods of impregnation.
[b] Crystal phases are listed in order of intensity. Brackets indicate trace amounts. HA = hexaaluminate, LAP = $LaAlO_3$, LAM = $LaAl_{1-X}Mn_XO_3$.
[c] Supported by the TPR analyses (see text).

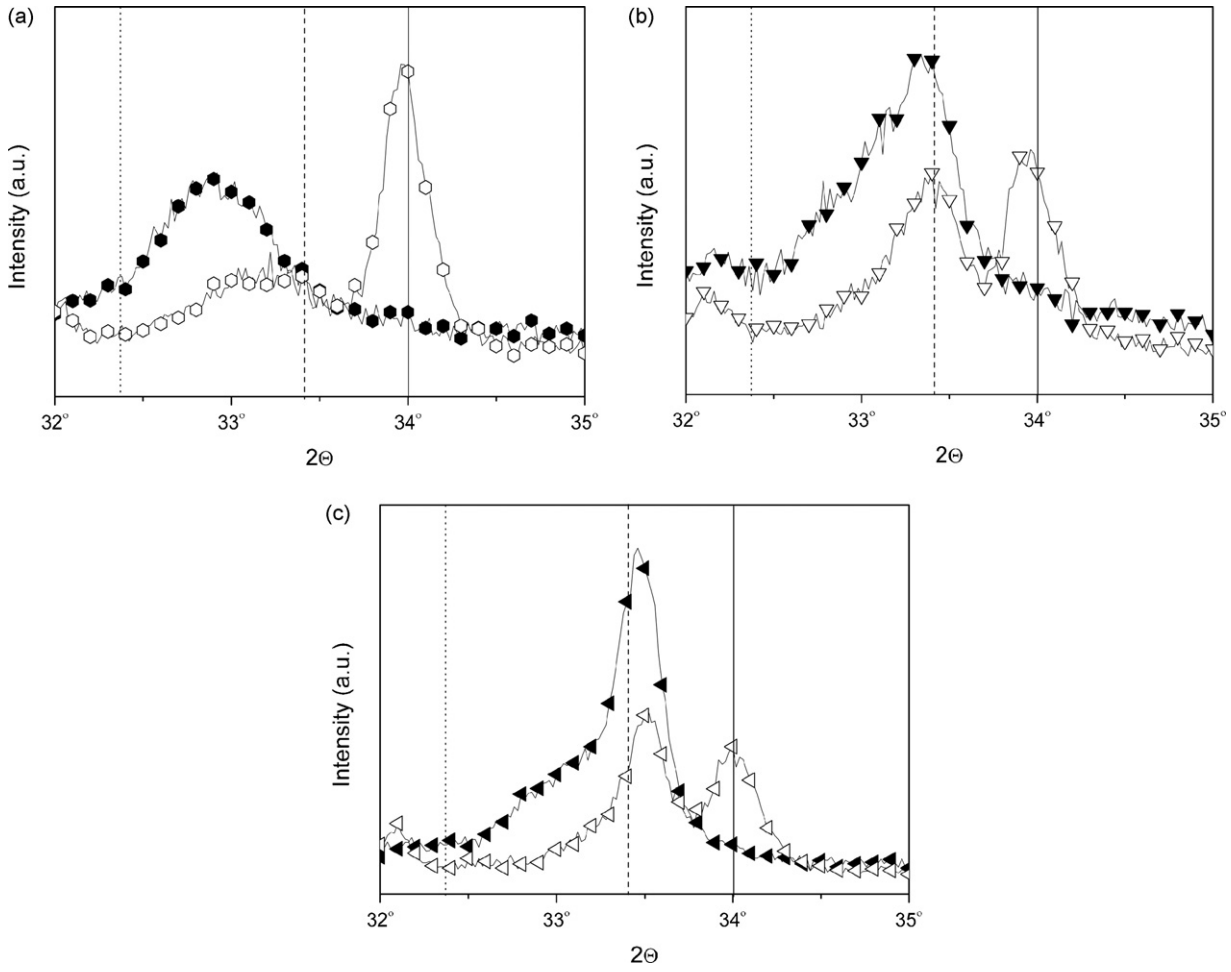

Fig. 3. X-ray diffractograms for the $LaMnO_3$ catalysts in their fresh state (filled symbols) and aged state (open symbols). LMP/Al_2O_3 (a), LMP/LHA (b), and LMP/LHA-150 (c). The dotted line indicates a $LaMnO_3$ reflection, the dashed line indicates a $LaAlO_3$ reflection and the solid line indicates a $LaAl_{11}O_{18}$ reflection.

precipitation, were calcined to the same temperature as the CeO_2 for all catalysts, i.e. 1000 °C. This assumption was tested by calcining a sample of Ce/LHA-SP at 1200 °C for 4 h. After this treatment, the same crystal phases of the support appeared with the same proportions as for the pure support (LHA), which indicates that the presence of CeO_2 does not interfere with the phase transformations of the LHA support. The average crystallite sizes of CeO_2 on the different supports, before and after aging, are shown in Table 3. Before aging it can be seen that the materials can be divided into two groups, one with crystallites around 10 nm and one with crystallites around 20 nm. Interestingly, one from each impregnation method (Ce/LHA-SP and Ce/LHA-150-IW) is represented in the group with the smaller crystallites. The crystallite sizes, before aging, calculated from XRD line broadening also agree fairly well with the transmission electron micrographs (TEM) displayed in Fig. 4a–d. However, separate CeO_2 particles were hard to identify in the materials prepared by surface precipitation, which could be expected from this preparation method where the aim is to disperse the cerium uniformly over the support. For Ce/LHA-SP (Fig. 4b), there are many particles considerably smaller than 12 nm, which was obtained from XRD. For Ce/LHA-150-SP (Fig. 4d), a broad size distribution of the CeO_2 particles was found, both above and below 22 nm, which was obtained from XRD. This might be due to the hydrothermal treatment of the microemulsion, which has unknown effects on the microemulsion system and especially the surfactant. This might have affected the impregnation process for Ce/LHA-150-SP. In opposite to the surface precipitation technique, the incipient wetness technique gave discrete CeO_2 particles with very uniform sizes (Fig. 4a and c).

Aging at 1000 °C for 100 h in humid air caused major sintering of the support for Ce/Al_2O_3, which resulted in the formations of large CeO_2 crystals (39 nm). Cerium did not inhibit the transformation into α-Al_2O_3 as lanthanum did in the case of LMP/Al_2O_3. This behavior is in agreement with previous findings, which was attributed to the fact that Ce^{3+} needed for the stabilization of alumina cannot be formed under oxidizing conditions [25]. The inability of cerium to switch to its trivalent state during the aging could also explain the low degree of interaction with the

Table 3
Average crystallite size of CeO_2 before and after aging at 1000 °C for 100 h in air with 10 vol.% H_2O

Identification code	Crystallite size (nm)	
	Fresh	Aged
Ce/Al_2O_3	22	39
Ce/LHA-IW	24	32
Ce/LHA-SP	12	17
Ce/LHA-150-IW	13	20
Ce/LHA-150-SP	22	33

The crystallite sizes were calculated with the Scherrer formula on the XRD reflection originating from the ⟨1 1 1⟩ crystal plane.

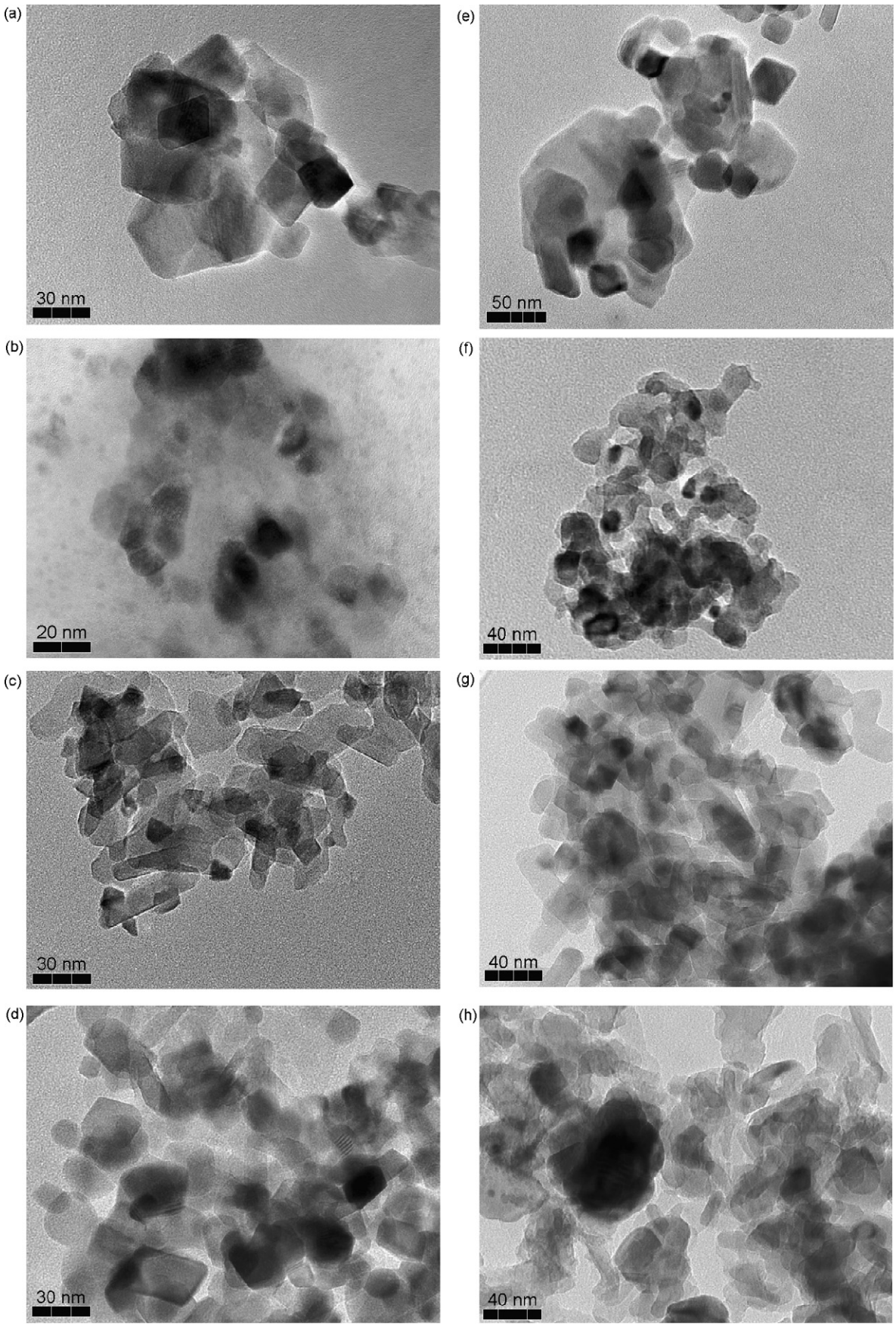

Fig. 4. Transmission electron micrographs (TEM), representative of the CeO_2 catalysts supported on lanthanum hexaaluminate (LHA). Fresh samples (a–d). Aged samples (e–h). Ce/LHA-IW (a and e), Ce/LHA-SP (b and f), Ce/LHA-150-IW (c and g), and Ce/LHA-150-SP (d and h).

LHA-based materials, since Ce^{4+} cannot replace La^{3+} in the crystal structure of lanthanum hexaaluminate and $LaAlO_3$. This could explain why the surface area of the Ce/LHA-150-IW to a large extent was retained after aging, which was not the case for the corresponding $LaMnO_3$ material (LMP/LHA-150). The two materials with the smallest CeO_2 crystallite sizes before aging, Ce/LHA-SP and Ce/LHA-150-IW, also had the smallest CeO_2 crystallites after aging (17 and 20 nm, respectively). For Ce/LHA-150-IW this may be explained by an almost intact support structure. This was however not the case for Ce/LHA-SP, for which the surface area decreased dramatically during aging. In the micrograph of Ce/LHA-SP (Fig. 4f) it appears that the CeO_2 particles are trapped in the support, which might give protection from sintering. For Ce/LHA-IW after aging, the CeO_2 particles are still present as discrete particles (Fig. 4e) of sizes agreeing well with that obtained from XRD. For Ce/LHA-150-SP, the broad size distribution of the CeO_2 particles, as seen before aging, were still present (Fig. 4h).

3.2. Redox properties

The redox properties of the catalysts are fundamental for the catalytic activities. The amount of excess oxygen (δ) in $LaMnO_{3+\delta}$, i.e. amount of Mn^{4+}, has been shown to be highly related to the oxidation activity [26]. Similarly, has increased reducibility of cerium from Ce^{4+} to Ce^{3+} shown to increase the activity for methane oxidation [18]. The reduction behaviors of both $LaMnO_3$ and CeO_2 have shown to be influenced by doping [24,27] and the reduction behavior could therefore give information concerning interaction between support and active component.

Table 4
Hydrogen consumption for the $LaMnO_3$ and CeO_2 catalysts expressed as fraction reduced of Mn^{4+} to Mn^{3+} and Ce^{4+} to Ce^{3+}, respectively

Identification code	Fraction reduced (%)	
	<600 °C	Total
LMP/Al_2O_3	28	37
LMP/LHA	28	40
LMP/LHA-150	25	33
Ce/Al_2O_3	26	71
Ce/LHA-IW	27	41
Ce/LHA-SP	18	102
Ce/LHA-150-IW	27	42
Ce/LHA-150-SP	16	84

The maximum temperatures used for the $LaMnO_3$ and CeO_2 catalysts were 800 and 950 °C, respectively.

The results from the hydrogen TPR analyses of the $LaMnO_3$ catalysts are shown in Fig. 5a. Quantitative analyses of the hydrogen consumptions are shown in Table 4. It has been shown by Cimino et al. [24] that the appearance of the TPR profile can give information about the amount of Al in the $LaAl_{1-X}Mn_XO_3$ solid

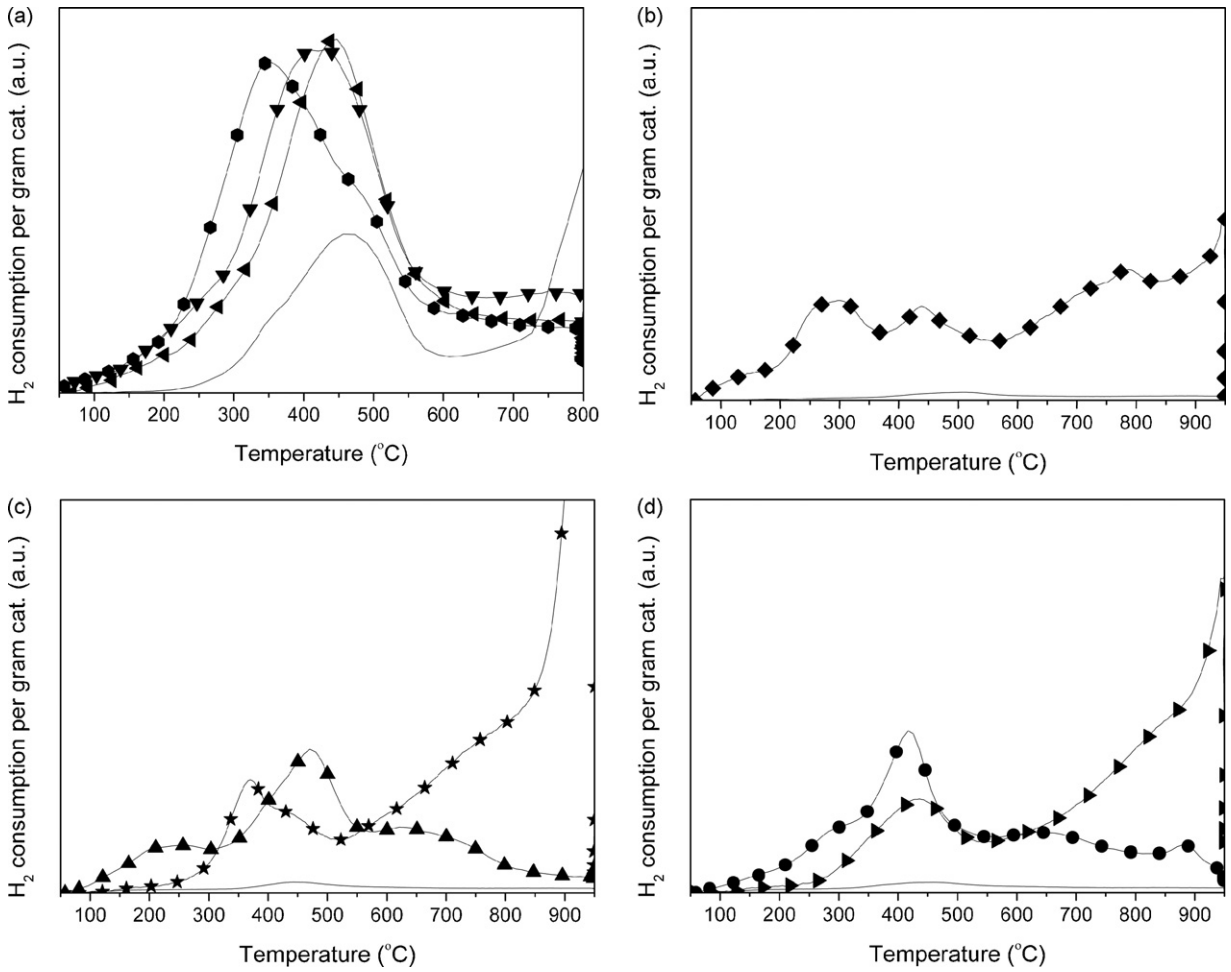

Fig. 5. Hydrogen TPR traces of the $LaMnO_3$ catalysts (a) and the CeO_2 catalysts (b–d). The scales of the hydrogen consumptions are the same for all CeO_2 catalysts. (a) LMP/Al_2O_3 (●), LMP/LHA (▼), LMP/LHA-150 (◀), pure $LaMnO_3$ (solid line). (b) Ce/Al_2O_3 (◆) and Al_2O_3 (solid line). (c) Ce/LHA-IW (▲), Ce/LHA-SP (★), and LHA (solid line). Note that the peak of hydrogen consumption for Ce/LHA-SP continues outside the graph. (d) Ce/LHA-150-IW (●), Ce/LHA-150-SP (▶), and LHA-150 (solid line).

solution, which in this case would be an indication of interaction between $LaMnO_3$ and the support. The authors showed that $LaAl_{1-X}Mn_XO_3$ was more stable towards reduction from Mn^{3+} to Mn^{2+} compared to pure $LaMnO_3$, indicated by lower hydrogen consumption at high temperature (800 °C). Furthermore, all $LaAl_{1-X}Mn_XO_3$ samples in the study by Cimino et al. were characterized by an increased reducibility of Mn^{4+} to Mn^{3+}, indicated by that the first peak of hydrogen consumption appeared about 100 °C lower compared to pure $LaMnO_3$. As seen in Fig. 5a, all samples showed the above-mentioned behaviors to some extent, thus supporting the results from XRD. The total hydrogen consumptions for all LMP catalysts were similar (Table 4). The fractions of Mn^{4+}, which was assumed to be responsible for the reduction below 600 °C, were 26–28%. These agree fairly well with the previously reported 35% [25].

The results from the hydrogen TPR analyses of the CeO_2 catalysts are shown in Fig. 5b–d. As seen, the supports were almost inert in the analyses and their contribution will therefore in the following be neglected. Quantitative analyses of the hydrogen consumptions are shown in Table 4. The reduction of pure ceria has been shown to occur in two steps, the first step occurs at around 500 °C and the second at around 800 °C [12,25]. The first reduction step has been attributed to the reduction of surface ceria and the second to bulk ceria [28]. The behavior during TPR analysis of ceria supported on Al_2O_3 has been reported to be similar as the behavior of pure ceria, with the difference that total reduction of Ce^{4+} to Ce^{3+} occurs below 1000 °C [25]. For pure ceria the total reduction was limited to around 50%. The result for Ce/Al_2O_3 (Fig. 5b) agrees fairly well with previously reported results [25], except that the reduction started already from the start of the analysis with an extra peak at 280 °C. The origin of this peak is not known, but could be the result of highly reducible surface species. Similarly, the reductions of the LHA catalysts prepared using the incipient wetness technique (Ce/LHA-IW, Ce/LHA-150-IW) also started at lower temperatures than reported for CeO_2 on Al_2O_3 (Fig. 5c and d, respectively). However, in these cases this could be due to doping by lanthanum from the supports. Lanthanum has previously been shown to enhance the reducibility of CeO_2 [18]. The low-temperature reductions (below 600 °C), which were attributed to the reductions of surface CeO_2, were for these three catalysts almost identical (Table 4). The total reduction during the analysis was however higher for Ce/Al_2O_3, which can be attributed to the higher surface area of the support in this case. The CeO_2 catalysts prepared by surface precipitation (Ce/LHA-SP, Ce/LHA-150-SP) showed quite different reduction behaviors (Fig. 5c and d, respectively). In opposite to the corresponding materials prepared by incipient wetness impregnation, these materials displayed TPR traces very similar to that of CeO_2 on Al_2O_3 previously reported [25]. These results are somewhat surprising, since surface precipitation of CeO_2 was expected to result in a very close contact with the support. Furthermore, the ceria was already present on the supports before calcination and the lanthanum in the supports was therefore expected to be more easily accessible. The surface precipitation catalysts also showed lower hydrogen consumptions below 600 °C, compared to the other catalysts (Table 4). On the other hand, the total amounts of consumed hydrogen for the surface precipitation catalysts were higher than for the other catalysts. In the case of Ce/LHA-SP, the amount of consumed hydrogen corresponds to total reduction of Ce^{4+}. This indicates that the CeO_2 was highly dispersed on this catalyst. The CeO_2 on Ce/LHA-150-SP was not fully reduced after completion of the analysis, which might be a result of the broad size distribution of the CeO_2 particles observed by TEM. The larger particles are likely harder to reduce.

3.3. Combustion activity

The catalytic activities of the catalytic materials coated on cordierite monoliths were evaluated in tests with 1.5 vol.% methane in air at a GHSV of 100,000 h^{-1}. During the activity tests, the $LaMnO_3$ catalysts generally gave CO_2 as the only detected product from oxidation of methane. The CeO_2 catalysts, on the other hand, always gave a small amount of CO when the conversion of methane was high. The amount of CO decreased under the detection limit only after full conversion of methane was reached. The threshold temperature over which homogenous reactions cannot be neglected was determined by testing a blank cordierite monolith (dotted line in Fig. 6a and b) in the activity test rig under the same conditions as the other activity tests. Below 800 °C the conversion from homogeneous reactions was very low, but substantial conversion was reached already at 825 °C.

The results from the activity tests of the $LaMnO_3$ catalysts before and after aging are shown in Fig. 6a. Manganese-substituted lanthanum hexaaluminate (LMHA) was included for comparison purposes. Before aging, the activities of the $LaMnO_3$ catalysts follow a trend of surface area. Higher surface area results in higher activity since higher surface area allows better dispersion of the $LaMnO_3$. LMP/Al_2O_3 was the most active catalyst, closely followed by LMHA. LMP/Al_2O_3 also retained its activity better during aging compared to the other catalysts, despite the changes in crystal structure observed with XRD. This might be connected to $LaAl_{1-X}Mn_XO_3$, which still was present after aging. This was not the case for any of the other catalysts. Aging resulted in deactivation of all catalysts presented in Fig. 6a, but the drop in activity was especially large for LMHA. This was not expected, since LMHA has been reported to be one of the most stable catalysts for high-temperature catalytic combustion [6]. Arai et al. [29] reported that a similar catalyst ($Sr_{0.8}La_{0.2}MnAl_{11}O_{19}$) experienced only minor deactivation after aging in powder form at 1300 °C in dry air for up to 6400 h. The authors contributed this to loss of surface area, which gradually decreased from 24 m^2/g initially to ~4 m^2/g after completion of the aging study. As seen in Table 2, this was not the case in the present study, since the surface area of LMHA remained unchanged after aging. Furthermore, in the same report Arai and co-workers reported that the amount of manganese in the sample remained constant during the course of aging. However, the same group reported in a later publication [30] that great differences of the manganese contents were found if the materials were aged in form of powder or coated on a surface. No differences in manganese contents, before and after aging, were found if the material was aged as powder, whereas a significant loss of manganese was recorded for a coated sample. Powder samples of LMHA in the present study, from before and after aging, also gave almost identical TPR profiles and total hydrogen consumptions. This suggests that the deactivation experienced by the LMHA during aging, only occurred when coated onto the monolith. Therefore, a sample of LMHA, taken from the coating of an aged monolith, was subjected to EDX analysis. Indeed, a lower content of manganese was measured in the aged sample (6.7 at.%) compared to the fresh sample (7.7 at.%). Hence, significant loss of manganese occurred in the present study already at 1000 °C, which is a surprisingly low temperature. This might be connected to the presence of 10 vol.% steam in the aging atmosphere, which previously has shown to greatly enhance evaporation of manganese due to the formations of volatile manganese hydroxides [5]. Furthermore, it was also revealed by EDX that the aged sample contained a considerable amount if silicon (0.5 at.%). Silicon released from the cordierite substrate has previously been shown to deactivate LMHA after calcination at 1200 °C for 4 h in dry air [31]. This process might be possible also at a lower temperature, as

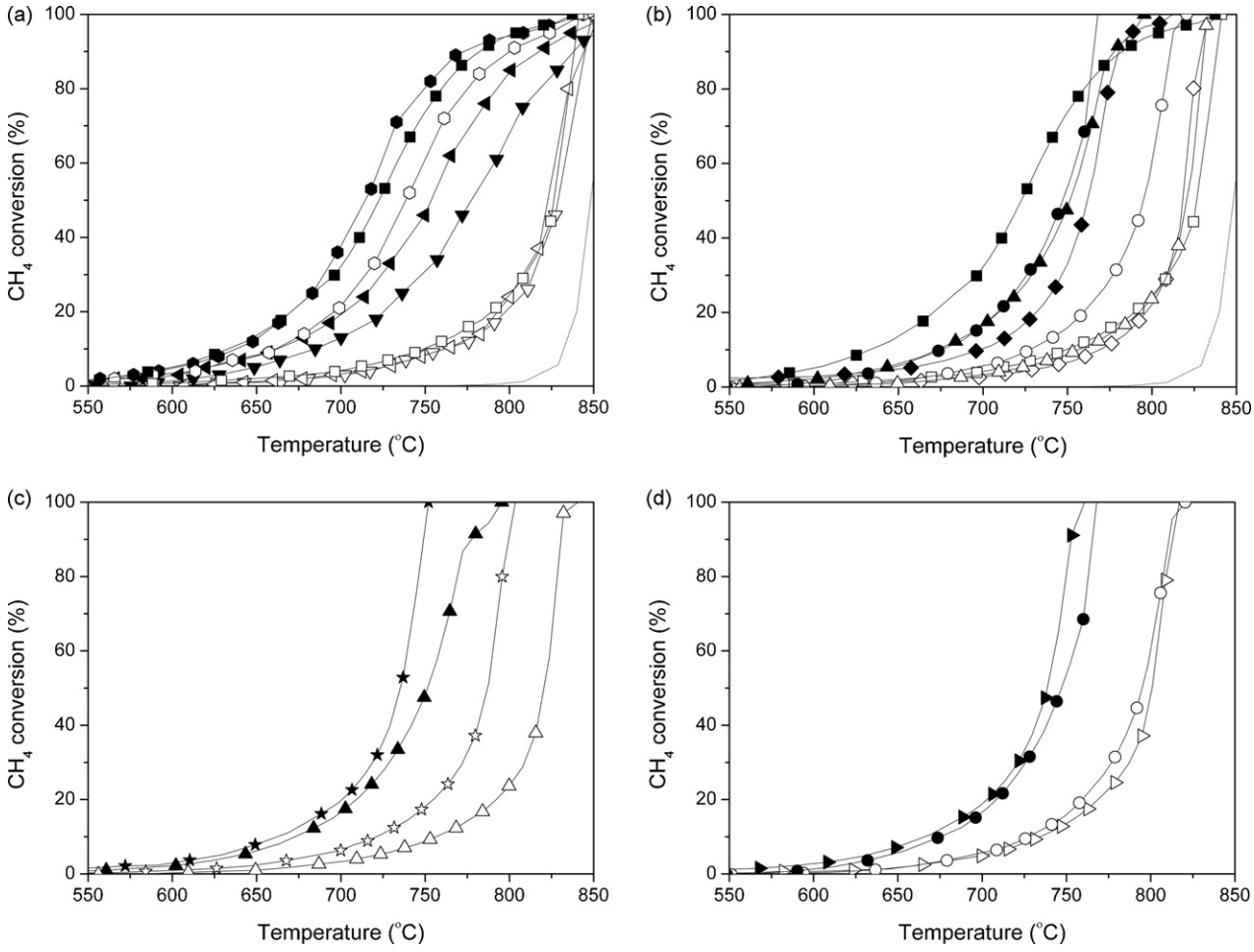

Fig. 6. Methane conversion for the $LaMnO_3$ catalysts (a) and the CeO_2 catalysts (b–d) coated onto cordierite monoliths. Filled symbols represent the fresh catalysts and open the aged catalysts. Gas composition: 1.5 vol.% CH_4 in air. GHSV = 100,000 h^{-1}. The dotted lines in (a) and (b) indicate blank monoliths. (a) LMP/Al_2O_3 (⬢), LMP/LHA (▼), LMP/LHA-150 (◀), and LMHA (■). (b) Ce/Al_2O_3 (◆), Ce/LHA-IW (▲), Ce/LHA-150-IW (●), LMHA (■). (c) Ce/LHA-IW (▲), and Ce/LHA-SP (★). (d) Ce/LHA-150-IW (●) and Ce/LHA-150-SP (▶).

in the present study, if the long duration and humid atmosphere are taken into account. The mobility of silicon has been shown to be greatly enhanced by the presence of water vapor [5]. Cordierite appears therefore not to be a suitable substrate material for LMHA, even if cordierite has been reported to be able to operate at temperatures as high as 1400 °C [32]. In similarity to the LMHA, the catalysts with $LaMnO_3$ supported on LHA deactivated strongly during aging. In fact, the activities of these three catalysts were almost identical. This might suggest that the deactivation mechanisms for the two LHA catalysts were the same as for LMHA, i.e. evaporation of manganese and silicon poisoning.

The results from the activity tests of the CeO_2 catalysts before and after aging are shown in Fig. 6b–d. Manganese-substituted lanthanum hexaaluminate (LMHA) was included in Fig. 6b for comparison purposes. Before aging, LMHA was the most active catalyst at the lower temperatures but above 750 °C the CeO_2 catalysts showed similar activity. Among the CeO_2 catalysts shown in Fig. 6b, Ce/LHA-IW and Ce/LHA-150-IW showed similar activity, the effect of the higher surface area of the latter was only obvious at high temperatures, where conversion of methane was high. Methane combustion over Ce/LHA-150-IW appeared to be kinetically controlled throughout the tested temperature range, whereas Ce/LHA-IW showed signs of mass-transfer limitations at high temperatures. Ce/Al_2O_3 showed the lowest activity among the catalysts, which might be explained by the fact that doping with lanthanum was not possible for the CeO_2 in this catalyst. It could also be the result of sintering of the support, which appeared to occur already during the catalyst preparation.

The drop in activities during aging for Ce/Al_2O_3 and Ce/LHA-IW were not as dramatic as for LMHA, but after aging the activities of these three catalysts were approximately the same. The loss of activity for Ce/Al_2O_3 was probably caused by sintering of the support, which leads to crystal growth of CeO_2. Also for Ce/LHA-IW, the crystal growth of CeO_2 was significant during aging, which could explain the drop in activity. Ce/LHA-150-IW deactivated considerably less than the other catalysts displayed in Fig. 6b. It appears that the higher surface area provided a better protection for the CeO_2 against crystal growth since the crystal size of CeO_2 was to a large extent retained after aging.

The influences of the impregnation methods on the activities before and after aging are shown in Fig. 6c and d. In Fig. 6c the activity tests for CeO_2 impregnated on non-hydrothermally treated LHA are shown. It is clear that the activity was enhanced by using the surface precipitation compared to incipient wetness. This could be explained both by the higher surface area of Ce/LHA-SP and the significantly smaller crystal size of CeO_2. The support of Ce/LHA-IW was pre-calcined at 1200 °C and was therefore expected to be more stable towards sintering during the aging. Indeed, the sintering of the support of Ce/LHA-IW was minimal during aging, but the activity dropped considerably more compared to Ce/LHA-SP. Despite that the surface area of Ce/LHA-SP dropped to almost half of its initial surface area (97–51 m^2/g), the deactivation was

less. In Fig. 6d the activity tests for CeO_2 impregnated on hydrothermally treated lanthanum hexaaluminate are shown. Before aging, the activity of Ce/LHA-150-SP was slightly higher than that of Ce/LHA-150-IW. Before testing Ce/LHA-150-SP, all activity tests with the CeO_2 catalysts have indicated the benefit of small CeO_2 crystallites. The fact that this catalyst displays such a high activity contradicts this relationship between the crystallite size and activity. This might be related to the broad size distribution of the CeO_2 particles in Ce/LHA-150-SP, which was observed with TEM. It is possible that the portion of small CeO_2 particles in this catalyst contributes to a large part of the activity. The same explanation might be valid after aging, after which the activity for Ce/LHA-150-SP was retained almost to the same level as for Ce/LHA-150-IW.

4. Conclusions

Lanthanum hexaaluminate (LHA) was successfully prepared through co-precipitation of metal nitrates within the water phase of a microemulsion. By subjecting the LHA precursor particles suspended in the microemulsion to hydrothermal treatment, a substantial increase of the surface area of the material was obtained after calcination at 1200 °C. This material as well as a non-hydrothermally treated material was used to support perovskite ($LaMnO_3$) and ceria (CeO_2). Both $LaMnO_3$ and CeO_2 were shown to be active catalysts for complete oxidation of methane.

The activity of the supported $LaMnO_3$ was shown to increase with increased surface area of the support. $LaMnO_3$ supported on the hydrothermally treated LHA was therefore more active than if supported on the non-treated LHA. For the same reason, was $LaMnO_3$ supported on the reference support (alumina) shown to be the most active catalyst in the study. This catalyst also showed high activity after aging at 1000 °C in humid air. Lanthanum (from $LaMnO_3$) played an important role in the stabilization of the alumina. $LaMnO_3$ was shown to interact with LHA negatively during aging, which led to strong deactivation. The same phenomenon was observed for manganese-substituted lanthanum hexaaluminate (LMHA). In this case, this was attributed to loss of manganese due to vaporization and silicon poisoning due to migration of silicon from the substrate (cordierite) into the LMHA. To the best of our knowledge, this has previously not been reported for LMHA or similar materials at such a low aging temperature as used in the present study. This highlights the importance of aging experiments with supported catalysts under realistic operating conditions.

The activity of the supported CeO_2 was shown to be almost independent of the surface area of the support. On the other hand, the nature of the support was shown to be important to retain small CeO_2 crystallites, which was shown to be important for a high activity. The importance of the support was apparent during aging. Alumina and the non-hydrothermally treated LHA gave poor protection against crystal growth of the CeO_2 particles and deactivated therefore strongly during aging. The LHA with higher surface area, obtained by hydrothermal treatment, deactivated considerably less during aging. Adding of CeO_2 to the support by precipitating cerium nitrate on the surface of the LHA precursor particles, while they still were suspended in the microemulsion, was shown to give catalysts with high activities. The activities of these catalysts were also retained to a large extent after aging.

Acknowledgements

The authors wish to express their gratitude for fundings from the European Union (CATHLEAN project, contract no.: ENK5-CT-2002-00683) and the Swedish energy agency (project 20419-2).

References

[1] M.F.M. Zwinkels, S.G. Järås, P.G. Menon, T.A. Griffin, Catal. Rev. Sci. Eng. 26 (1993) 319.
[2] L.D. Pfefferle, W.C. Pfefferle, Catal. Rev. Sci. Eng. 29 (1987) 219.
[3] P. Forzatti, Catal. Today 83 (2003) 3.
[4] R. Carroni, V. Schmidt, T. Griffin, Catal. Today 75 (2002) 287.
[5] J.G. McCarty, M. Gusman, D.M. Lowe, D.L. Hildenbrand, K.N. Lau, Catal. Today 47 (1999) 5.
[6] G. Groppi, G. Cristiani, P. Forzatti, Catalysis 13 (1997) 85.
[7] M. Machida, K. Eguchi, H. Arai, J. Catal. 120 (1989) 377.
[8] P. Ciambelli, S. Cimino, S. De Rossi, M. Faticanti, L. Lisi, G. Minelli, I. Pettiti, P. Porta, G. Russo, M. Turco, Appl. Catal. B: Environ. 24 (2000) 243.
[9] S. Cimino, S. Colonna, S. De Rossi, M. Faticanti, L. Lisi, I. Pettiti, P. Porta, J. Catal. 205 (2002) 309.
[10] M. Haneda, T. Mizushima, N. Kakuta, A. Ueno, Bull. Chem. Soc. Jpn. 67 (1994) 2617.
[11] S. Cimino, L. Lisi, R. Pirone, G. Russo, M. Turco, Catal. Today 59 (2000) 19.
[12] C. Bozo, N. Guilhaume, E. Garbowski, M. Primet, Catal. Today 59 (2000) 33.
[13] M.F.M. Zwinkels, O. Haussner, P. Govind Menon, S.G. Järås, Catal. Today 47 (1999) 73.
[14] P.E. Marti, M. Maciejewski, A. Baiker, in: G. Poncelet, et al. (Eds.), Preparation of Catalysts VI, 1995, p. 617.
[15] E. Elm Svensson, M. Lualdi, M. Boutonnet, S.G. Järås, in: K. Eguchi, et al. (Eds), Stud. Surf. Sci. Catal. 172 (2007) 465.
[16] S. Eriksson, U. Nylén, S. Rojas, M. Boutonnet, Appl. Catal. A: Gen. 265 (2004) 207.
[17] A.J. Zarur, J.Y. Ying, Nature 403 (2000) 65.
[18] Lj. Kundakovic, M. Flytzani-Stephanopoulos, J. Catal. 179 (1998) 203.
[19] H. Arai, M. Machida, Appl. Catal. A: Gen. 138 (1996) 161.
[20] B.J. Palla, D.O. Shah, P. Garcia-Casillas, J. Matutes-Aquino, J. Nanopart. Res. 1 (1999) 215.
[21] A.G. Ersson, E.M. Johansson, S.G. Järås, In B. Delmon, et al. (Eds.), Stud. Surf. Sci. Catal. 118 (1998) 601.
[22] G. Groppi, C. Cristiani, P. Forzatti, Appl. Catal. B: Environ. 35 (2001) 137.
[23] M.F.M. Zwinkels, S. Druesne, P.G. Menon, E. Björnbom, S.G. Järås, Ind. Eng. Chem. Res. 37 (1998) 391.
[24] S. Cimino, L. Lisi, S. De Rossi, M. Faticanti, P. Porta, Appl. Catal. B: Environ. 43 (2003) 397.
[25] A. Piras, A. Trovarelli, G. Dolcetti, Appl. Catal. B: Environ. 28 (2000) L77.
[26] P. Porta, S. De Rossi, M. Faticanti, G. Minelli, I. Pettiti, L. Lisi, M. Turco, J. Solid State Chem. 146 (1999) 291.
[27] A. Trovarelli, Catal. Rev.-Sci. Eng. 38 (1996) 439.
[28] V. Perrichon, A. Laachir, G. Bergeret, R. Frety, L. Tournayan, O. Touret, J. Chem. Soc., Faraday Trans. 90 (1994) 773.
[29] H. Arai, K. Eguchi, M. Machida, T. Shiomitsu, in: S. Yoshida, et al. (Eds.), Catal. Sci. Technol., Proc. Tokyo Conf. 1st, 1991, p. 195.
[30] H. Inoue, K. Sekizawa, K. Eguchi, H. Arai, Catal. Today 47 (1999) 181.
[31] A. Ersson, PhD Thesis, KTH, TRITA-KET R176, 2003.
[32] D.L. Trimm, Appl. Catal. 7 (1983) 249.